Toxicology Research

Accepted Manuscript

ROYAL SOCIETY OF CHEMISTRY

www.rsc.org/toxicology

Full Title: PROMISING BLOOD-DERIVED BIOMARKERS FOR ESTIMATION OF *POSTMORTEM* INTERVAL

Running Head: Estimation of *postmortem* interval

Authors' names and institutional addresses:
Isabel Costa[1,2,3*], Félix Carvalho[2], Teresa Magalhães[3,4], Paula Guedes de Pinho[3], Ricardo Silvestre[5,6*], Ricardo Jorge Dinis-Oliveira[1,2,3,4*]

[1]IINFACTS - Institute of Research and Advanced Training in Health Sciences and Technologies, Department of Sciences, Advanced Institute of Health Sciences – North (ISCS-N), CESPU, CRL, Gandra, Portugal.
[2]UCIBIO-REQUI*M*TE, Laboratory of Toxicology, Department of Biological Sciences, Faculty of Pharmacy, University of Porto, Porto, Portugal.
[3]Department of Legal Medicine and Forensic Sciences, Faculty of Medicine, University of Porto, Porto, Portugal.
[4]CENCIFOR - Forensic Sciences Center, Coimbra, Portugal.
[5]Life and Health Sciences Research Institute (ICVS), School of Health Sciences, University of Minho, Braga, Portugal.
[6]ICVS/3B's – PT Government Associate Laboratory, Braga/Guimarães, Portugal.

*Corresponding authors:

Ricardo Jorge Dinis-Oliveira: ricardinis@med.up.pt
Ricardo Jorge Leal Silvestre: ricardosilvestre@ecsaude.uminho.pt
Department of Legal Medicine and Forensic Sciences,
Faculty of Medicine, University of Porto,
Jardim Carrilho Videira, 4050-167 Porto, Portugal.
Phone: +351 222073850

ACKNOWLEDGEMENTS

Ricardo Dinis-Oliveira acknowledges Fundação para a Ciência e a Tecnologia (FCT) for his Investigator Grant (IF/01147/2013).

ABSTRACT

A precise estimation of the *postmortem* interval (PMI) is one of the most important topics in forensic pathology. However, the PMI estimation is based mainly on the visual observation of cadaverous phenomena (*e.g. algor*, *livor* and *rigor mortis*) and on alternative methods such as thanatochemistry that remain relatively imprecise. The aim of this *in vitro* study was to evaluate the kinetic alterations of several biochemical parameters (*i.e.* proteins, enzymes, substrates, electrolytes and lipids) during putrefaction of human blood. For this purpose, we performed a kinetic biochemical analysis during a 264 hour period. Results showed a significant linear correlation between total and direct bilirubin, urea, uric acid, transferrin, immunoglobulin M (IgM), creatine kinase (CK), aspartate transaminase (AST), calcium and iron with the time of blood putrefaction. These parameters allowed us to develop two mathematical models that may have predictive value and become important complementary tools of traditional methods to achieve a more accurate PMI estimation.

Keywords: *postmortem* interval; blood putrefaction changes; forensic pathology; biochemical parameters.

INTRODUCTION

One of the most important and challenging problems for forensic pathologists is the accurate estimation of the *postmortem* interval (PMI) [1]. The main subjacent principle is the calculation of a measurable date along a time-dependent curve back to the starting point [2]. All the methods currently used to estimate the PMI are still far from being exact. The physical (*algor mortis*, *livor mortis*) and physicochemical (*rigor mortis*) changes comprise the main basis for PMI estimation, especially during the first hours after death. However, these changes have limitations in PMI determination, due to the bias inflicted by several variables [3-8]. Others methods such as thanatochemistry and molecular techniques have been reported, attempting for a more accurate PMI estimation, but until now all these methods are also relatively inexact and/or poorly reproducible [9]. Over the last few decades, some progress in PMI estimation has been

made using biochemical parameters, supported by different statistical approaches [9-11]. These methods have been shown to be more accurate in PMI estimation, since the effect of external conditions is less relevant than in the currently used traditional methods. Moreover, a combination of traditional and biochemical methods has been proposed to increase the reliability of PMI estimations and narrow down the margins of error associated to individual analysis [9,12,13]. An important feature of biochemical methods is also the possibility of using results for accurate estimation of PMI during the first days after death since most victims are found in the first hours after death [9]. Abstract Figure summarizes the current methods used for PMI estimation.

An accurate estimation of the PMI requires the evaluation of parameters that correlate with time after death [14]. This definition fits well in *postmortem* changes of biochemical parameters, since each change has its own time factor. These changes begin immediately after death, initiating at the cellular level and subsequently evolving to hemolysis, discoloration, swelling, putrefaction, among other processes [15,16]. During human decomposition, several biochemical changes take place in all body tissues due to the absence of circulating oxygen and the consequent cessation of aerobic respiration, altered enzymatic reactions, cessation of anabolic production of metabolites, active membrane transport stops and changes in the permeability of cells and diffusion of ions [5,17-19]. The catabolic activity of key enzymes on proteins, lipids, carbohydrates and nucleic acids and the rate of this process may be used to estimate the PMI [15,17,19-21]. Additionally, the leaching of electrolytes, and blood pH changes, due to accumulation of several ions and metabolites such as bicarbonate, carbon dioxide, hydrogen ions, lactate, phosphoric and formic acid have been suggested as potential targets for PMI determination [17,22].

Biochemical analysis as a useful indicator for estimating PMI has already been presented by some authors. Data reported a significant correlation between the *postmortem* concentration of some biochemical parameters such as potassium [1,11,23-25], urea [26], glucose [11,23], lactate [17], hypoxanthine [17,24,27], glycated hemoglobin [28], calcineurin A, phosphatase 2A [8,29], troponin [30], cytochrome *c* oxidase [31], lactate and malate dehydrogenase [32], gamma amino butyric acid [15] and PMI in distinct biological matrices (*e.g.* vitreous humor, blood, cerebrospinal and synovial fluids).

The development of more reliable techniques will certainly represent important tools to be used in the court of law (*e.g.* by inclusion or exclusion of possible suspects) [33]. Therefore, this study aims to evaluate the kinetic alterations of 46 biochemical

parameters in human blood in order to develop a mathematical model that could be used as a complementary procedure for the methodologies already used. Thus, substrates, proteins, enzymes, electrolytes and lipids are targeted in this study, since these may be useful for rigorous PMI estimation.

MATERIALS AND METHODS

Samples

Twenty independent human venous blood samples (40 mL each) were collected from healthy donors and divided for 16 plastic tubes (*e.g.* without anticoagulant or any other additive), one for each of the defined endpoints (see below). Informed written consent was obtained from the participants. This work was also approved by the Ethical Commission of the Faculty of Medicine of University of Porto/Saint John Hospital. Whole blood was submitted to a temperature gradual decrease from 37 to 21ºC, mimicking the decline of body temperature after death until it reaches room temperature. According to the literature [13], there is an initial maintenance of body temperature that may last for a few hours, followed by a relatively linear rate of *postmortem* cooling, until reaching room temperature. Thus, during the first hour, samples were maintained at 37ºC in a thermostatic bath. Then, the temperature was decreased 0.5˚C/hour up to 12h, 1ºC/hour up to 18h and 0.5ºC/hour until room temperature was achieved.

Quantitative pH and biochemical parameters kinetic analysis

Determination of the pH and the quantification of the vast biochemical array (46) of different biochemical parameters was performed at 16 defined endpoints to promote hemolysis (1, 4, 8, 12, 14, 24, 48, 72, 96, 120, 144, 168, 192, 216, 240, 264 hours). For that, complete venous blood samples and then centrifuged at 3000 *g* for 10 min to obtain serum. The following biochemical parameters were quantified in this study using a PRESTIGE 24i® automated Chemistry analyzer: substrates [urea, creatinine, uric acid, lactate, glucose, direct bilirubin and total bilirubin (Cormay, Poland)], enzymes [lipase,

creatine kinase – (CK)-MB and NAC izoenzymes (Spinreact, Spain), creatine kinase (CK), γ-glutamyl transpeptidase (γ-GT), lactate dehydrogenase (LDH), alanine transaminase (ALT), aspartate transaminase (AST), alkaline phosphatase (ALP), acid phosphatase (ACP), pseudocholinesterase, ceruloplasmin and amylase (Cormay, Poland)], proteins [albumin, total protein, C-reactive protein (CRP), α_1-antitrypsin, immunoglobulins A, M, G and E (IgA, M, G and E), complement C3 and C4, ferritin, transferrin (Cormay, Poland) and β_2-microglobulin (Spinreact, Spain)], lipids [cholesterol, triglycerides (Cormay, Poland), phospholipids, high-density lipoprotein (HDL) and low-density lipoprotein (LDL) (Spinreact, Spain)], electrolytes [calcium, magnesium, iron, phosphorus (Cormay, Poland), sodium, potassium, chloride and zinc (Spinreact, Spain)]. A very brief description is given below:

Bilirubin was converted to colored azobilirubin by diazotized sulfanilic acid. Color intensity is proportional to the bilirubin concentration in the sample and was measured photometrically at 555 nm. Of the two fractions present in serum (*i.e.* bilirubin glucuronide and free bilirubin loosely bound to albumin), only conjugated bilirubin reacts directly in aqueous solution (direct bilirubin), while free bilirubin requires solubilization with dimethylsulphoxide to react (indirect bilirubin). The concentration of indirect bilirubin = total bilirubin - direct bilirubin.

Lactate was oxidized by lactate oxidase to pyruvate and hydrogen peroxide which, in the presence of peroxidase, reacts with N-ethyl-N-(2-hydroxy-3-sulfopropyl)-3-methylaniline forming a red compound that was measured at 546 and 700 nm. Glucose oxidase catalyzes the oxidation of glucose to gluconic acid. The formed hydrogen peroxide was detected by a chromogenic oxygen acceptor, phenol-4-aminophenazone in the presence of peroxidase. The intensity of the quinone color formed was measured photometrically at 505 nm. Creatinine reacted with alkaline picrate forming a red complex that was measured photometrically at 492 nm. Urea in the sample reacted with *o*-fhthalaldehyde in acid medium forming a colored complex that was measured photometrically at 510 nm. Uric acid was oxidized by uricase to allantoine and hydrogen peroxide, which under the influence of peroxidase, 4-aminophenazone and 2-4 dichlorophenol sulfonate formed a red quinoneimine compound that was measured photometrically at 520 nm.

Calcium quantification was based by formation of color complex with *o*-cresolphtalein in alkaline medium that was measured photometrically at 570 nm. Chloride formed a red ferric thiocyanate complex with mercuric thiocyanate that was

measured photometrically at 480 nm. Iron was dissociated from transferring-iron complex in weakly acid medium. Liberated iron was reduced to ferrous form by ascorbic acid and formed a colored complex with FerroZine that was measured photometrically at 562 nm. Magnesium formed a colored complex when reacted with magon sulfonate in alkaline solution. The intensity of the color formed is proportional to the magnesium concentration in the sample and was measured photometrically at 546 nm. Phosphorus reacted with molybdic acid forming a phosphomolybdic complex. Its subsequent reduction in alkaline medium originated a blue molybdenum color that was measured photometrically at 710 nm. Potassium ions reacted with sodium tetraphenylboron in a protein-free alkaline medium to produce a finely dispersed turbid suspension of potassium tetraphenyylboron. The turbidity produced is proportional to the potassium concentration and was read photometrically at 578 nm. Sodium was determined enzymatically via sodium dependent-galactosidase activity with *o*-nitrophenyl-β-galactoside as substrate. The absorbance at 405 nm of the product *o*-nitrophenyl is proportional to the sodium concentration. Zinc reacted at pH 8.6, in a buffered media, with a specific complexant 5-Br-PAPS, to form a stable colored complex that was measured photometrically at 560 nm.

Cholesterol originated a colored complex in the presence of peroxidase that was measured photometrically at 505 nm. Phospholipids were hydrolyzed by phospholipase D and the liberated choline was subsequently oxidized by choline oxidase to betaine with the simultaneous production of hydrogen peroxide. In the presence of peroxidase the hydrogen peroxide couples oxidatively the 4-aminophenazone and dichlorophenol to form a quinonemine dye that is measured photometrically at 505 nm. Triglycerides were converted to glycerol and free fatty acids by lipoprotein lipase. Glycerol was converted to glycerol-3-phosphate and ADP by glycerol kinase and ATP. Glycerol-3-phosphate was then converted by glycerol phosphate dehydrogenase to dihydroxyacetone phosphate and hydrogen peroxide. In the last reaction, hydrogen peroxide reacted with 4-aminophenazone and *p*-chlorophenol in presence of peroxidase to give a red colored dye that is measured photometrically at 505 nm. HDL and LDL originate a colored complex in the presence of peroxidase that was measured photometrically at 600 nm.

ACP catalyses the hydrolysis of α-naphthylphosphate liberating the α-naphthol and phosphate. The α-naphthol was then coupled with diazotised 4-chloro-2-methylbenzene (Fast Red TR) to form a diazo dye which was measured photometrically at 405 nm. ALP catalyzes the hydrolysis of *p*-nitrophenyl phosphate at pH 10.4, liberating

phosphate and *p*-nitrophenol, which was measured photometrically at 405 nm. Amylase hydrolyzes the 2-chloro-4-nitrophenyl-α-D-maltotrioside to release 2-chloro-4-nitrophenol and form 2-chloro-4-nitrophenyl-α-D-maltoside, maltotriose and glucose. The rate of 2-chloro-4-nitrophenol formation is proportional to the activity of amylase present in the sample and was measured photometrically at 405 nm. Pseudocholinesterase hydrolyze butyrylthiocholine to butyrate and thiocholine. Thiocholine reacts with 5,5'-dithiobis-2-nitrobenzoic acid to form 5-mercapto-2-nitrobenzoic acid, which the formation rate was measured photometrically at 405 nm. CK catalyzes the reversible transfer of a phosphate group from phosphocreatine to ADP. This reaction is coupled to those catalyzed by hexokinase and glucose-6-phosphate dehydrogenase. The rate of NADPH formation is proportional to the catalytic concentration of CK present in the sample and was measured photometrically at 340 nm. γ-GT catalyzes the transfer of γ-glutamyl group from γ-glutamyl-p-nitroanilide to acceptor glycylglycine. The rate of 2-nitro-5-aminobenzoic acid formation is proportional to the catalytic concentration of γ-GT present in the sample and was measured photometrically at 405 nm. AST catalyzes the reversible transfer of an amino group from aspartate to α-ketoglutarate forming glutamate and oxalacetate. The oxalacetate produced was reduced to malate by malate dehydrogenase using NADH as cofactor. ALT catalyzes the reversible transfer of an amino group from alanine to α-ketoglutarate forming glutamate and piruvate. The piruvate produced was reduced to lactate by LDH using NADH as cofactor. LDH catalyzes the reduction of pyruvate to lactate using NADH as cofactor. The rate of decrease in concentration of NADH is proportional to the activity of AST, ALT and LDH present in the sample and was measured photometrically at 340 nm. Lipase in presence of colipase, desoxycholate and calcium ions, hydrolyses the substrate 1-2-O-dilauryl-rac-glycero-3-glutaric acid-(6'-methylresorufin)-ester. The rate of methylresorufin formation was measured photometrically at 580 nm.

Total proteins gave an intensive violet-blue complex with copper salts in an alkaline medium that was measured photometrically at 546 nm. Iodide was included as an antioxidant. Albumin in the presence of bromocresol green at a slightly acid pH, produced a color change of the indicator from yellow-green to green-blue. The intensity of the color formed is proportional to the albumin concentration in the sample and was measured photometrically at 605 nm.

C3, C4, α_1-antritrypsin, ceruloplasmin, transferrin, CRP, β_2-microglobulin, IgA, IgG, IgM and IgE form insoluble complexes when mixed with respective antibodies. These complexes cause a turbidity change, dependent upon C3, C4, α_1-antritrypsin, ceruloplasmin, transferrin, CRP, β_2-microglobulin, IgA, IgG, IgM and IgE concentrations in the sample. Concentrations can be quantified by comparison with a calibrator of know C3, C4, α_1-antritrypsin, ceruloplasmin, transferrin, CRP, β_2-microglobulin, IgA, IgG, IgM and IgE concentration.

Blood pH was determined using a micro-electronic pH meter Sigma-Aldrich (St Louis, MO, USA). Certified calibration buffer standards Sigma-Aldrich (St Louis, MO, USA) were used before each pH analysis.

Data analysis

Quantification and expression data were statistically processed using GraphPad Prism 6. The determined *p* values of the statistical significance were examined using the model of linear regression and the Pearson correlation (r). An acceptable Pearson correlation value of r>0.900 was considered for posterior analysis. Mathematical model was developed from the 264 hour kinetics, by performing regression analysis using Tool Analysis supplement of Microsoft Excel 2013 for Windows, in order to estimate the slope (m) and *y*-intercept (b) errors. Level of significance was always set to *p*-value less than 0.05 ($p<0.05$).

RESULTS

Quantitative pH and kinetic analysis of biochemical parameters

The concentrations of biochemical parameters were analyzed in 20 different human blood samples to establish a potential relationship between these values and the putrefaction time aiming to identify those that present good correlations. A statistically significant increase was observed in the urea concentration between 27.84-33.49 mg/dL up to 264 h (r=0.973, $p<0.001$) (Figure S1). Acid uric concentration decreased until 264 h between 3.39-2.80 mg/dL and showed a strong correlation (r=-0.980, $p<0.001$) with

the putrefaction time (Figure S1). The total and direct bilirubin concentrations significantly decreased over the time from 0.67-0.30 mg/dL and from 0.14-0.01 mg/dL, respectively (r=-0.964 and r=-0.991, $p<0.001$) (Figure S1). Our data demonstrate that the remaining substrates (*i.e.* glucose, lactate and creatinine) did not correlate linearly with putrefaction time (Figure S2). Among the electrolytes, the calcium concentration decreased significantly and linearly from 8.45 to 3.70 mg/dL (r=-0.986, $p<0.001$) (Figure S1). A statistically significant increase was observed in the iron concentration between 100.72-188.49 µg/dL over the putrefaction time (r=0.987, $p<0.001$) (Figure S1). The remaining electrolytes (*i.e.* zinc, sodium, potassium, magnesium and phosphorus) did not correlate linearly (Figure S2) or exhibited several fluctuations with putrefaction time (*i.e.* chloride) (Figure S3). Among the lipids (*i.e.* phospholipids, lipoprotein HDL and LDL, triglycerides and cholesterol), we did not observe any linear correlation between each of the parameters and the putrefaction time (Figure S2). Of all proteins evaluated in this study, only transferrin and IgM proved to be useful for PMI estimation (Figure S1). Transferrin concentration decreased significantly and linearly between 340.64-275.09 mg/dL (r=-0.988, $p<0.001$) with the putrefaction time. IgM concentration decreased linearly from 112.37-103.00 (r=-0.967, $p<0.001$). The remaining proteins (*i.e.* total protein, albumin, complements C3 and C4, IgA and G, ferritin, β_2-microglobulin, α_1-antitrypsin and CRP) did not correlate linearly (Figure S2) or exhibited several fluctuations with putrefaction time (*i.e.* IgE) (Figure S3). The changes in the activity of several enzymes were also evaluated *in vitro*. AST concentration increased significantly and linearly between 25.23-40.75 U/L (r=0.980, $p<0.001$) over time (Figure S1). CK concentration also increased significantly between 108.95-190.39 U/L with putrefaction time (r=0.968, $p<0.001$) (Figure S1). Our data demonstrate that the remaining enzymes (*i.e.* ALT, amylase, pseudocholinesterase, ALP, CK-MB isoenzyme, γ-GT, LDH and lipase) did not correlate linearly (Figure S2) or exhibited several fluctuations with putrefaction time (*i.e.* ceruloplasmin, ACP and CK-NAC izoenzyme) (Figure S3).

Aiming to assure the maximum significance between each biochemical parameter and the putrefaction time, we considered for posterior analysis only those with Pearson correlations higher than 0.900 (*i.e.* in absolute value or modulus) and found to be statistically significant (Figure 1). This approach allowed the identification of 10 potential biochemical parameters in the blood as the most reliable dependent variables that may correlate with PMI:

- Positive slope - iron, urea, AST and CK;

- Negative slope - total and direct bilirubin, uric acid, transferrin, IgM and calcium.

At each defined endpoint, the samples were also analyzed for pH, since after death several mechanisms may be involved in producing the pH changes [22]. In our study, the pH decreased very slightly in the first 5 days compared to the initial value (pH 7.45 to 7.10). Afterwards, the pH increased continuously reaching pH 7.74 by the end of the experiment.

Development of a mathematical model with predictive value for PMI estimation

The ultimate goal of this study was to develop a mathematical model to correlate biochemical parameters with PMI. In that sense, we performed regression analysis with the objective of building descriptive mathematical laws to be used by forensic experts for valid and reliable estimation of the PMI. The linearity of the method was determined by evaluation of the regression curve (biochemical parameter concentration *versus* time) and expressed by the correlation coefficient (*r*) as previously proposed [14]. We used 20 independent calibration curves (y = mx + b) for each of the 10 selected biochemical parameters to obtain the mean slopes (m) and y-intercept (b). Linearity was accepted if r $\geq$ 0.900. Nonlinear parameters were excluded from our model. The goal of linear regression was to determine the best estimates for the slope and y-intercept. This was accomplished by minimizing the residual error between the experimental *y* values, and those values predicted by regression line equation. The most commonly used form of linear regression is based on three assumptions: (1) differences between the experimental data and the calculated regression line is due to indeterminate errors affecting the *y* values, (2) indeterminate errors are normally distributed, and (3) that the indeterminate errors in *y* do not depend on the value of *x*. The derivation of equations for calculating the estimated slope and *y*-intercept can be found elsewhere [34]. This allows us to define regression equations to calculate the PMI using the parameters with positive and negative slope (Figure 2, equations A and B, respectively). Once known, it is possible to determine the PMI and to estimate the error associated to time. For that, we can measure an average signal for our sample ($\overline{Y}_x$) and use it to calculate the value of *x*. The PMI should be calculated by the mean of the two equations. The standard deviation for the calculated value of *x* (S_x) is given by the equation in Figure 2, equation

C, where K is the number of replicate samples (K=20) used to establish $\overline{Y}_x$, n is the number of measured endpoint times (n=16), $\overline{y}$ is the average signal for each endpoint time, $\sum xx$ is the summation of individual $(x-\overline{x})^2$. Once S_x is known, the confidence interval for the PMI can be calculated attending the value of t determined by the desired level of confidence (p<0.05) for n - 2 degrees of freedom.

DISCUSSION

The results of this study allowed us to circumscribe the potential biomarkers (total and direct bilirubin, urea, uric acid, transferrin, immunoglobulin M, creatine kinase, aspartate aminotransferase, calcium and iron) for accurately estimating PMI. These biochemical parameters were then used to develop mathematical models with predictive value for the accurate estimation of the PMI.

After death, several biochemical alterations occur. Blood glucose concentrations decrease very rapidly after death with a concomitant increase of lactate concentrations [35-37]. Indeed, *postmortem* lactate concentrations were shown to be up to 60 times higher than *antemortem* [37]. In our study, lactate concentration progressively increased over the time while glucose decreased rapidly up to 144 h. Interestingly, an increased glucose concentration over the remaining putrefaction time was registered. Since during the human decomposition progresses, cell membranes gradually disintegrate as a result of autolysis and putrefaction processes [38,39], the *postmortem* glucose concentrations may increase in blood [40]. *In situ*, besides autolysis, glycogen is metabolized to glucose (*i.e.* glycogenolysis namely in liver), which is released into the blood [40,41]. Additionally, glucose may also be formed from non-carbohydrate sources (*e.g.* lactate, amino acids and glycerol) by gluconeogenesis, contributing to the increase of glucose after death.

Creatinine is a degradation product of phosphocreatine (*i.e.* an energy storage molecule in muscle), which is released into the blood [41-43]. Our study shows that creatinine concentration increase abruptly until the 24 h and then stabilize over the remaining PMI. In previous studies, creatinine showed a tendency to increase in *postmortem* blood *in situ* up to 48 h [28]. A strong correlation was found in muscle [44], and there were no significant changes in other specimens such as synovial fluid and vitreous humor [11].

We found a significant increase of urea concentration over time, which corroborates other studies performed with *postmortem* blood [35,45]. However, in other specimens, such as vitreous humor and synovial fluid, urea was shown to remain relatively stable [9,11]. *In situ*, amino acids are oxidized, nitrogen is then released as ammonia and converted mainly to urea in liver, passing into the blood. Upon degradation of pyrimidine bases, the carbon and nitrogen atoms produce carbon dioxide and urea, respectively [41,43]. Thus, an accumulation of ammonia and urea due to amino acid and nucleotide catabolism is a natural consequence of *postmortem* decomposition [17]. Uric acid is also an excretion product containing nitrogen, but is derived from purine bases of nucleic acids and not from protein [41]. The purine degradation produces hypoxanthine, which is oxidized by xanthine oxidase to uric acid [1,41]. *Postmortem* enzymatic activity is inhibited, since it requires oxygen to function [17,46,47]. In this study, uric acid concentration decreased linearly with putrefaction time. However, some previous studies have shown that blood uric acid remained relatively steady *in vitro* while decreased in blood *in situ* [17,48].

Total and direct bilirubin concentrations *in vitro* also significantly and linearly decrease with putrefaction time. Our results can be explained by the activity of bacterial β-glucuronidases to remove glucuronide groups and then reducing bilirubin (produced by heme oxidation) to urobilinogen and stercobilinogen [41]. Nevertheless, a stability or even a slightly increase of total bilirubin was registered during the first 4-5 endpoints. These results are somewhat in accordance with the findings of Uemura and colleagues [28] using right cardiac blood obtained from autopsies. Indeed, these authors observed a non-significant increase of total bilirubin up to 72 h, but they did not extend their study beyond that endpoint. Moreover, cadavers were preserved refrigerated until forensic autopsies and therefore could not be straightly compared with our findings. In order to minimize the influence of the preservation time in a refrigerated environment for PMI estimation, blood should be collected quickly after the body is found and not only when the autopsy begins.

Analysis of *postmortem* chemical changes of electrolytes have been extensively studied by several authors with promising results. Indeed, good correlations with PMI have been observed for potassium and sodium, which were shown to increase and decrease respectively, in vitreous humor [1,10,11,25,49-51]. In our study, potassium concentration increased significantly up to 168 h and decreased over the remaining putrefaction time. Sodium concentration *in vitro* initially stayed stable up to 72 h, but decreased significantly with the putrefaction time. Sodium is the most abundant cation

in the extracellular space, while potassium is prevalent in the intracellular space [52]. These ions are essential for cellular function, namely for the maintenance of membrane potential and regulation of osmotic pressure [43,52]. After death, cells lose their normal morphology as a result of autolysis and putrefaction processes [39]. Thus, *in vitro*, the increase in extracellular potassium concentration in blood results mainly from loss of potassium from blood cells (namely erythrocytes), and *in situ*, can also result from cells located in the vessels' walls and extravascular tissues [53]. In this study, we found a linear and significant increase of the iron concentration *in vitro* over the putrefaction time. These findings can be explained by the *postmortem* leakage of iron from erythrocytes due to hemolysis and release from transferrin. Accordingly, we observed that transferrin concentration decreases significantly and linearly with the putrefaction time. The iron storage protein, ferritin [41,52], initially exhibited an increase, but decreased with putrefaction time after 72 h.

Other electrolytes such as phosphorus, calcium, magnesium, zinc and chloride, have been also studied by some authors mainly in the vitreous humor and synovial fluid [11,25,54,55]. It was demonstrated that electrolytes concentrations do not change significantly with putrefaction time. However, others observed a significant correlation between these electrolytes concentration and PMI [4,33,45,56]. Our data shows that, similar to potassium, phosphorus concentration increased gradually up to 168 h, but decreased slightly over the remaining putrefaction time. Chloride revealed to be a very unstable parameter over the putrefaction time and therefore was excluded. Magnesium concentration increased *in vitro* up to 96 h and stayed practically constant over the remaining putrefaction time. Zinc concentration increased until 120h and then decreased slightly. Calcium concentration decreased significantly and linearly with the putrefaction time. Calcium plays an important role in the regulation of many cellular processes (*e.g.* blood coagulation, muscle contraction and secretory processes) [41,52]. In this regard, we hypothesize that the observed calcium decrease was due to consumption during the coagulation process and was retained in the fibrin coagulum.

Few studies correlate the concentration of lipids with PMI. The blood lipoproteins HDL and LDL are involved in transport of lipids from the liver to other tissues in the body [42,52,57]. LDL is the main carrier of lipids (*e.g.* triglycerides and cholesterol) from the liver to peripheral tissues (such as muscle) and to adipose tissue [52,58]. HDL is involved in reverse transport of lipids from peripheral tissues to the liver [42,52,58]. In our

study, the lipoproteins LDL and HDL concentrations initially increase slightly, but then showed a tendency to decrease over the time.

Triglycerides concentration *in vitro* showed a tendency to decrease over time. *In situ*, it was also observed a *postmortem* decrease of triglycerides concentration, since these are hydrolyzed in the blood to fatty acids and glycerol by lipoprotein lipase [41,52]. In the adipose tissue, triglycerides are degraded and supply fatty acids and glycerol to liver and muscle. There they can be used for gluconeogenesis or are directly oxidized [52]. The cholesterol and phospholipids concentrations *in vitro* showed a tendency to increase up to 48 h and then decreased slightly, with some oscillations over the time. Sarkioja and colleagues [18] reported that unpredictable fluctuations occur in plasma triglycerides and cholesterol concentrations within 24 h after death. Previously Uemura *et al.* [28] showed a significant time-dependent decrease in triglycerides concentration up to 72 h after death and cholesterol concentration registered some fluctuations.

During *postmortem* decomposition, proteins are broken down via enzymatic processes into proteoses, peptones, polypeptides, and amino acids [59,60]. Liver function is maintained for several hours after death as shown by the ability to carry out protein synthesis at low levels despite *postmortem* conditions [61]. Some authors have proposed PMI estimation based on the effect of PMI on protein concentration [8,28-30,62,63]. Accordingly to our results, total protein concentration initially increased, up to 48 h, reaching a plateau that remain unchanged until the end of the experiment. Albumin concentration *in vitro* increased slightly up to 216 h and then decreased over the remaining putrefaction time. β_2-microglobulin is a protein located on the surface of nucleated cells such as lymphocytes [52]. Our results, shown that β_2-microglobulin concentrations did not change significantly with increasing putrefaction time.

The α_1-antitrypsin concentration decreased during the first 4h remaining stable over the rest of the experiment. α_1-antitrypsin is a circulating protein synthesized by the liver and the most abundant proteinase inhibitor in plasma that down regulates inflammation [41,52,58]. We observed that C-reactive protein, a non-specific indicator of acute phase response in trauma, myocardial infarction, tumors, infection and other inflammatory changes, decreased gradually with putrefaction time in our experimental setting. The site of this protein synthesis and release is mainly in the liver [64]. Uhlin-Hansen [65] compared *ante*- and *postmortem* concentrations of C-reactive protein and reported that the *postmortem* concentration of this protein reduced approximatelly 35%. In another

study, C-reactive protein concentration was stable in *postmortem* blood for at least 2 days, suggesting its biochemical stability [64].

C3 and C4 complement concentrations increased up to 96 h and decreased over the remaining putrefaction time. The estimation of PMI based on the third component of C3 cleavage was previously studied in *postmortem* blood, where a significant positive correlation between percentage of C3 cleavage and PMI was found [62]. Additionally, we observed a decrease of immunoglobulin G and M concentrations with putrefaction time. However, immunoglobulin A concentration remained practically constant up to 120 h, decreasing over the remaining time. E immunoglobulin showed to be a very unstable parameter to be considered for putrefaction time estimation.

The determination of enzyme activity for estimation of PMI was previously presented by some authors [28,31,32,61,66-69]. Some enzymes continue to operate for some time after death (*e.g.* ACP, ALP, esterase, β-glucuronidase), while others rapidly lose their activity (*e.g.* due to pH alterations) within 24-36 h of the autolysis start (*e.g.* succinic dehydrogenase, cytochrome oxidase) [70,71].

Some hours after death, autolysis releases intracellular enzymes (*e.g.* proteases, lipases, amylases) into blood [36]. The erythrocytes have high concentrations of AST and LDH enzymes and hemolysis can elevate its *postmortem* concentrations [66]. This study demonstrates that AST increases significantly with putrefaction time. The ALT concentration also increases, although not significantly, since high concentrations are only found in liver and kidney. The LDH is an important enzyme, which catalyzes a step in anaerobic glucose metabolism and glucose synthesis in skeletal muscle, liver and erythrocytes [17,42]. LDH concentration *in vitro* decreased slightly during the first 24 h and then increased with putrefaction time. *In situ*, with the tissues decomposition and autolysis (*e.g.* liver and skeletal muscle cells) allows enzymes to leak into the blood and therefore it is expected an increase of transaminases, LDH, ALP and ACP concentrations [41,43]. However, in our study, the ALP concentration *in vitro* decreased over the time. This enzyme is present in high concentrations in liver, bone, intestine and kidney but not in blood cells [58], therefore hemolysis of these cells will not have much influence on the concentration and enzyme activity decreases rapidly in the blood. ACP is an enzyme present in the erythrocytes and hemolysis can elevate its concentration in the blood. High concentrations of this enzyme are particularly found in the prostate and liver [58]. In this study, ACP proved to be a very unstable parameter over the putrefaction time. The γ-GT concentration *in vitro* stayed relatively stable up to 192 h, decreasing

over the remaining putrefaction time. This is a cellular enzyme that is particularly present in high levels in the liver, kidney and pancreas [58]. γ-GT shows a tendency to increase towards *postmortem* in a time-dependently manner, though not significantly in *postmortem* blood [11].

We also found that CK concentration correlates significantly with putrefaction time. The concentration of CK-MB izoenzyme increases slightly up to 96 h and more pronounced over the remaining putrefaction time. CK-NAC isoenzyme proved to be a very unstable parameter for PMI estimation. CK is found in higher concentrations in the muscle cells. CK catalyzes the transfer of phosphate from adenosine triphosphate to creatine, to form phosphocreatine. The *in vitro* results demonstrated that this enzyme remained active over time, since the creatinine is a degradation product from phosphocreatine and increased over time. *In situ*, there is an increase of CK (namely MB isoenzyme of CK) *postmortem* concentration due to a release of this enzyme into the blood from cell lysis in the heart muscle and necrotic tissue after death. *In vitro*, the ceruloplasmin also was an unstable parameter over the putrefaction time. Ceruloplasmin is a serum enzyme that contains copper, synthesized mainly by the hepatic cells and is involved in the oxidation of iron so it can be transported [41,43].

Amylase concentration stayed relatively stable *in vitro* up to 120 h, decreasing significantly over the remaining time. The amylase enzyme is produced mainly by pancreas and salivary glands. This enzyme may leak into the blood due to the lysis of pancreatic cells, being expected an increase of *postmortem* concentration *in situ*. Lipase concentration *in vitro* decreased slightly and stayed relatively stable up to 264 h, with some oscillations over the time. Lipase is a pancreatic enzyme that hydrolyzes triglycerides to fatty acids and glycerol [41,52]. The pseudocholinesterase is an enzyme that is present in blood, but is synthesized in the liver. *In vitro*, pseudocholinesterase concentration remained practically constant up to 216 h and decreased over the remaining time. In a previous study [28] this enzyme showed a tendency to decrease time-dependently in *postmortem* blood.

At each defined endpoint, the blood samples were also analyzed for pH, since after death several mechanisms (*e.g.* autolysis, putrefaction) may be involved, resulting in pH modifications [22]. In our study, the pH decreased very slightly compared to initial values (pH 7.45 to 7.10) and then increased to 7.74 until the limit of our study. Similarly, Donaldson and Lamont [17] performed an *in vitro* study with blood samples from rats and humans and verified that pH only decreased slightly (pH 7.4 to 7.1) relatively to an *in*

situ study (pH 7.4 to 5.1) over a 96 hour period. Our hypothesis is that, *in vitro*, the autolysis and putrefactive process does not occur as extensively as *in situ* and consequently the blood cells are degraded more slowly over time. In cadavers, several compounds are released into the blood resulting from the putrefactive alterations in organs. Therefore, the accumulation of acidic metabolites is much more significant *in situ* and the blood pH decreases more rapidly. This decline in pH values does not continue indefinitely. Indeed, it was also previously reported that pH starts to rise after approximately four days [19,71,72].

The results of this study impelled us to develop a mathematical model to describe the behavior of the identified biochemical parameters over PMI as a valuable tool for forensic pathologists. Only total and direct bilirubin, urea, uric acid, transferrin, IgM, CK, AST, calcium and iron biochemical parameters were considered, since Pearson correlations were higher than 0.900 (*i.e.* in absolute value or modulus). For the purpose of generating the formulas to estimate the PMI, it was calculated the mean concentrations of parameters with negative slope (*i.e.* total and direct bilirubin, uric acid, transferrin, IgM and calcium) and the mean concentrations of parameters with positive slope (*i.e.* iron, urea, AST and CK). Thus, two formulas were generated. For estimating the PMI in real samples, the average signals obtained from selected parameters with positive and negative slope ($\overline{Y}_x$) are used to calculate the value of *x*. The PMI should be calculated by the mean of the two equations. This mathematical model can thus be considered a promising easy approach for PMI estimation.

CONCLUSIONS

It is expected that the current study may provide a new paradigm for estimation of PMI and become a complementary procedure for the methodologies already used. It is important to mention that the proposed model can match the most common found environmental conditions after death. Indeed, we followed the *postmortem* decline of the body temperature model previously described by Siegel [13]. However, this model is influenced by internal (or intrinsic) and external (or extrinsic), *antemortem* and *postmortem* conditions. Age (*e.g.* low fluid levels of elderly inhibit the growth of microorganisms and delays decomposition), gender (*e.g.* abundant subcutaneous fatty tissue of females retains body heat for a longer period and decomposition is

accelerated), xenobiotic administration, cause of death (*e.g.* hanging may influence the levels of potassium and hypoxantine in vitreous humor), body mass (*e.g.* an obese will form adipocere more readily and thus delays the decomposition) and duration of agonal state are some internal factors that may influence the estimation of PMI [3-5]. Regarding external factors, environment temperature, humidity, rain, clothing (acts as a barrier that delays decomposition), location of the body (*e.g.* a body buried in soil is less influenced by oxidative processes by the lack of oxygen and will decomposed at a significantly slower rate than if exposed to air) and insect or animal activity have been reported to influence the estimation of PMI [6-8]. Therefore, the initial value as well as the slope of the curve will depend on many factors, which means that estimation of the time since death only reveals a certain period of time, but not a precise time point. Nevertheless, it was impossible to attain all potential variables and therefore this represents a preliminary study that must be further validated using laboratory animals and then with human *in situ* samples.

FIGURE LEGENDS

Figure 1 - Mean graphical concentrations of the biochemical parameters (n=20) analyzed during a 264 hours kinetic period. A - Parameters with negative slope (*i.e.* total and direct bilirubin, uric acid, transferrin, immunoglobulin M and calcium); B - Parameters with positive slope (*i.e.* iron, urea, aspartate transaminase and creatine kinase). Pearson correlation (r) and *p* value are depicted.

Figure 2 - Mathematical models for the accurate estimation of the PMI. The two equations represent the formula to calculate the PMI using parameters with positive (A) and negative (B) slopes, with a confidence interval of 95% and the standard deviation (C), where ($\overline{Y}_x$) is the average signal for our sample, *K* is the number of replicate samples used to establish $\overline{Y}_x$, *n* is the number of measured endpoint times, $\overline{y}$ is the average signal for each endpoint time, $\sum xx$ is the summation of (individual x - $\overline{x}$)^2. The mean result of the A and B formulas allow us to determine the PMI.

Figure S1 - Standard curves of linear biochemical parameters (n=20) analyzed during a 264 hours kinetic period.

Figure S2 - Standard curves of non-linear biochemical parameters (n=20) analyzed during a 264 hours kinetic period.

Figure S3 - Biochemical parameters (n=20) analyzed during a 264 hours kinetic period that showed to exhibit too much fluctuations to be fitted to a standard curve.

REFERENCES

1. Passos ML, Santos AM, Pereira AI, et al. Estimation of postmortem interval by hypoxanthine and potassium evaluation in vitreous humor with a sequential injection system. Talanta 2009;79:1094-9.
2. Madea B. Handbook of Forensic Medicine. Oxford: John Wiley & Sons, Ltd; 2014.
3. Zhu BL, Ishikawa T, Michiue T, et al. Differences in postmortem urea nitrogen, creatinine and uric acid levels between blood and pericardial fluid in acute death. Legal medicine 2007;9:115-22.
4. Singh D, Prashad R, Parkash C, Sharma SK, Pandey AN. Double logarithmic, linear relationship between plasma chloride concentration and time since death in humans in Chandigarh Zone of North-West India. Legal medicine 2003;5:49-54.
5. Madea B, Musshoff F. Postmortem biochemistry. Forensic science international 2007;165:165-71.
6. Ferreira MT, Cunha E. Can we infer post mortem interval on the basis of decomposition rate? A case from a Portuguese cemetery. Forensic science international 2013;226:298 e1-6.
7. Vass AA. The elusive universal post-mortem interval formula. Forensic science international 2011;204:34-40.
8. Poloz YO, O'Day DH. Determining time of death: temperature-dependent postmortem changes in calcineurin A, MARCKS, CaMKII, and protein phosphatase 2A in mouse. International journal of legal medicine 2009;123:305-14.
9. Munoz Barus JI, Febrero-Bande M, Cadarso-Suarez C. Flexible regression models for estimating postmortem interval (PMI) in forensic medicine. Stat Med 2008;27:5026-38.
10. Munoz JI, Suarez-Penaranda JM, Otero XL, et al. A new perspective in the estimation of postmortem interval (PMI) based on vitreous. J Forensic Sci 2001;46:209-14.
11. Tumram NK, Bardale RV, Dongre AP. Postmortem analysis of synovial fluid and vitreous humour for determination of death interval: A comparative study. Forensic science international 2011;204:186-90.
12. Madea B. Is there a recent progress in the estimation of postmortem interval by means of thanatochemistry? Forensic Sci Int 2005;151:139–49.

13. Siegel JA, Saukko PJ, Knupfer GC. Encyclopedia of Forensic Sciences. London: Academic Press2000.
14. Sampaio-Silva F, Magalhaes T, Carvalho F, Dinis-Oliveira RJ, Silvestre R. Profiling of RNA degradation for estimation of post morterm interval. PloS one 2013;8:e56507.
15. Vass AA, Barshick SA, Sega G, et al. Decomposition chemistry of human remains: a new methodology for determining the postmortem interval. J Forensic Sci 2002;47:542-53.
16. Sasaki S, Tsunenari S, Kanda M. The estimation of the time of death by non-protein nitrogen (NPN) in cadaveric materials. Report 3: multiple regression analysis of NPN values in human cadaveric materials. Forensic science international 1983;22:11-22.
17. Donaldson AE, Lamont IL. Biochemistry Changes That Occur after Death: Potential Markers for Determining Post-Mortem Interval. PLoS ONE 2013;8:e82011.
18. Sarkioja T, Yla-Herttuala S, Solakivi T, Nikkari T, Hirvonen J. Stability of plasma total cholesterol, triglycerides, and apolipoproteins B and A-I during the early postmortem period. J Forensic Sci 1988;33:1432-8.
19. Boumba VA, Ziavrou KS, Vougiouklakis T. Biochemical pathways generating post-mortem volatile compounds co-detected during forensic ethanol analyses. Forensic science international 2008;174:133-51.
20. Lehninger AL. Principles of biochemistry: New York, Worth Publishers; 1982.
21. Statheropoulos M, Agapiou A, Spiliopoulou C, Pallis GC, Sianos E. Environmental aspects of VOCs evolved in the early stages of human decomposition. Sci Total Environ 2007;385:221-7.
22. Sawyer WR, Steup DR, Martin BS, Forney RB. Cardiac blood pH as a possible indicator of postmortem interval. Journal of forensic sciences 1988;33:1439-44.
23. Madea B, Kreuser C, Banaschak S. Postmortem biochemical examination of synovial fluid--a preliminary study. Forensic Sci Int 2001;118:29-35.
24. Munoz Barus JI, Suarez-Penaranda J, Otero XL, et al. Improved estimation of postmortem interval based on differential behaviour of vitreous potassium and hypoxantine in death by hanging. Forensic Sci Int 2002;125:67-74.
25. Jashnani KD, Kale SA, Rupani AB. Vitreous humor: biochemical constituents in estimation of postmortem interval. J Forensic Sci 2010;55:1523-7.
26. Prieto-Castello MJ, Hernandez del Rincon JP, Perez-Sirvent C, et al. Application of biochemical and X-ray diffraction analyses to establish the postmortem interval. Forensic Sci Int 2007;172:112-8.
27. Lendoiro E, Cordeiro C, Rodriguez-Calvo MS, et al. Applications of Tandem Mass Spectrometry (LC-MSMS) in estimating the post-mortem interval using the biochemistry of the vitreous humour. Forensic Sci Int 2012;223:160-4.
28. Uemura K, Shintani-Ishida K, Saka K, et al. Biochemical blood markers and sampling sites in forensic autopsy. J Forensic Leg Med 2008;15:312-7.
29. Kang S, Kassam N, Gauthier ML, O'Day DH. Post-mortem changes in calmodulin binding proteins in muscle and lung. Forensic Sci Int 2003;131:140-7.
30. Sabucedo AJ, Furton KG. Estimation of postmortem interval using the protein marker cardiac Troponin I. Forensic Science International 2003;134:11-6.
31. Ikegaya H, Iwase H, Hatanaka K, et al. Postmortem changes in cytochrome c oxidase activity in various organs of the rat and in human heart. Forensic science international 2000;108:181-6.

32. Gos T, Raszeja S. Postmortem activity of lactate and malate dehydrogenase in human liver in relation to time after death. Int J Legal Med 1993;106:25-9.
33. Mathur A, Agrawal YK. An overview of methods used for estimation of time since death. Australian Journal of Forensic Sciences 2011;43:275–85.
34. Draper NR, Smith H. Applied Regression Analysis. 3nd ed. Wiley: New York1998.
35. Naumann HN. Postmortem chemistry of the vitreous body in man. Arch Ophthalmol 1959;62:356-63.
36. Forrest AR. Obtaining samples at post mortem examination for toxicological and biochemical analyses. Journal of Clinical Pathology 1993;46:292-6.
37. Karlovsek MZ. Diagnostic values of combined glucose and lactate values in cerebrospinal fluid and vitreous humour--our experiences. Forensic Sci Int 2004;146 Suppl:S19-23.
38. Kugelberg FC, Jones AW. Interpreting results of ethanol analysis in postmortem specimens: a review of the literature. Forensic science international 2007;165:10-29.
39. Dokgoz H, Arican N, Elmas I, Fincanci SK. Comparison of morphological changes in white blood cells after death and in vitro storage of blood for the estimation of postmortem interval. Forensic Sci Int 2001;124:25-31.
40. Corry JE. A review. Possible sources of ethanol ante- and post-mortem: its relationship to the biochemistry and microbiology of decomposition. J Appl Bacteriol 1978;44:1-56.
41. Lieberman MA, Ricer R. Biochemistry, Molecular Biology, and Genetics. Philadelphia. Lippincott Williams & Wilkins. 2014.
42. Berg JM, Tymoczko JL, Stryer L. Biochemistry. New York. W. H. Freeman and Company2012.
43. Pelley JW. Elsevier's integrated Biochemistry. Philadelphia. Mosby, Elsevier 2007.
44. Brion F, Marc B, Launay F, Gailledreau J, Durigon M. Postmortem interval estimation by creatinine levels in human psoas muscle. Forensic Sci Int 1991;52:113-20.
45. Drolet R, D'Allaire S, Chagnon M. The evaluation of postmortem ocular fluid analysis as a diagnostic aid in sows. J Vet Diagn Invest 1990;2:9-13.
46. Bocaz-Beneventi G, Tagliaro F, Bortolotti F, Manetto G, Havel J. Capillary zone electrophoresis and artificial neural networks for estimation of the post-mortem interval (PMI) using electrolytes measurements in human vitreous humour. Int J Legal Med 2002;116:5-11.
47. Madea B, Käferstein H, Hermann N, Sticht G. Hypoxanthine in vitreous humour and cerebrospinal fluid - a marker of postmortem interval and prolonged (vital) hypoxia? Remarks also on hypoxanthine in SIDS. Forensic Sci Int 1994;65:19-31.
48. Zhu BL, Ishida K, Quan L, et al. Postmortem serum uric acid and creatinine levels in relation to the causes of death. Forensic Sci Int 2002;125:59-66.
49. Mulla A, Kalra J. Vitreous Humour Biochemical Constituents - Evaluation of eye differences. Am J Forensic Med Pathol 2005;26:146-9.
50. Madea B, Henssge C, Honig W, Gerbracht A. References for determining the time of death by potassium in vitreous humor. Forensic science international 1989;40:231-43.
51. Balasooriya BA, St Hill CA, Williams AR. The biochemistry of vitreous humor. A comparative study of the potassium, sodium and urate concentrations in the eyes at identical time intervals after death. Forensic Sci Int 1984;26:85–91.
52. Michal G, Schomburg D. Biochemical Pathways: An Atlas of Biochemistry and Molecular Biology. Canada. John Wiley & Sons, Inc.2012.

53. Querido D. In vitro loss of potassium from erythrocytes during the 0-108 h postmortem period in rats: relationship between potassium loss and postmortem interval. Forensic Sci Int 1991;51:111-23.
54. Madea B, Hermann N, Henssge C. [Calcium concentration in vitreous humor--a means for determining time of death?]. Beitr Gerichtl Med 1990;48:489-99.
55. Farmer JG, Benomran F, Watson AA, Harland WA. Magnesium, potassium, sodium and calcium in post-mortem vitreous humour from humans. Forensic Sci Int 1985;27:1-13.
56. Querido D. Linearization of the relationship between postmortem plasma chloride concentration and postmortem interval in rats. Forensic Sci Int 1990;45:117– 27.
57. Timbrell JA. Principles of Biochemical Toxicology. Informa Healthcare USA, Inc.2009.
58. Wilson K, Walker J. Principles and Techniques of Biochemistry and Molecular Biology. United Kingdom. Cambridge University Press 2010.
59. Hoffman EM, Curran AM, Dulgerian N, Stockham RA, Eckenrode BA. Characterization of the volatile organic compounds present in the headspace of decomposing human remains. Forensic Sci Int 2009;186:6-13.
60. Dekeirsschieter J, Verheggen FJ, Gohy M, et al. Cadaveric volatile organic compounds released by decaying pig carcasses (Sus domesticus L.) in different biotopes. Forensic Sci Int 2009;189:46-53.
61. Nunley WC, Schuit KE, Dickie MW, Kinlaw JB. Delayed, in vivo hepatic post-mortem autolysis. Virchows Arch B Cell Pathol 1972;11:289-302.
62. Kominato Y, Harada S, Yamazaki K, Misawa S. Estimation of postmortem interval based on the third component of complement (C3) cleavage. J Forensic Sci 1988;33:404-9.
63. Miura M, Naka T, Miyaishi S. Postmortem changes in myoglobin content in organs. Acta medica Okayama 2011;65:225-30.
64. Fujita MQ, Zhu BL, Ishida K, Quan L, Oritani S, Maeda H. Serum C-reactive protein levels in postmortem blood--an analysis with special reference to the cause of death and survival time. Forensic Sci Int 2002;130:160-6.
65. Uhlin-Hansen L. C-reactive protein (CRP), a comparison of pre- and post-mortem blood levels. Forensic Sci Int 2001;124:32-5.
66. Buras KL. Are enzymes accurate indicators of postmortem interval? A biochemical analysis.: B.S., Louisiana State University.; 2006.
67. Kooij A, Schijns M, Frederiks WM, Van Noorden CJ, James J. Distribution of xanthine oxidoreductase activity in human tissues--a histochemical and biochemical study. Virchows Arch B Cell Pathol Incl Mol Pathol 1992;63:17-23.
68. Fahn S, Cote LJ. Stability of enzymes in post-mortem rat brain. J Neurochem 1976;26:1039-42.
69. Karkela JT. Critical evaluation of postmortem changes in human autopsy cisternal fluid. Enzymes, electrolytes, acid-base balance, glucose and glycolysis, free amino acids and ammonia. Correlation to total brain ischemia. J Forensic Sci 1993;38:603-16.
70. Evans WED. The chemistry of death. Springfield: Charles C Thomas. 1963.
71. Butzbach DM. The influence of putrefaction and sample storage on post-mortem toxicology results. Forensic Sci Med Pathol 2010;6:35-45.
72. Schleyer F. Determination of the time of death in the early post-mortem interval. In: F. Lindquist (ed.), Methods of Forensic Science. New York: Interscience Publishers; 1963.

Figure 1

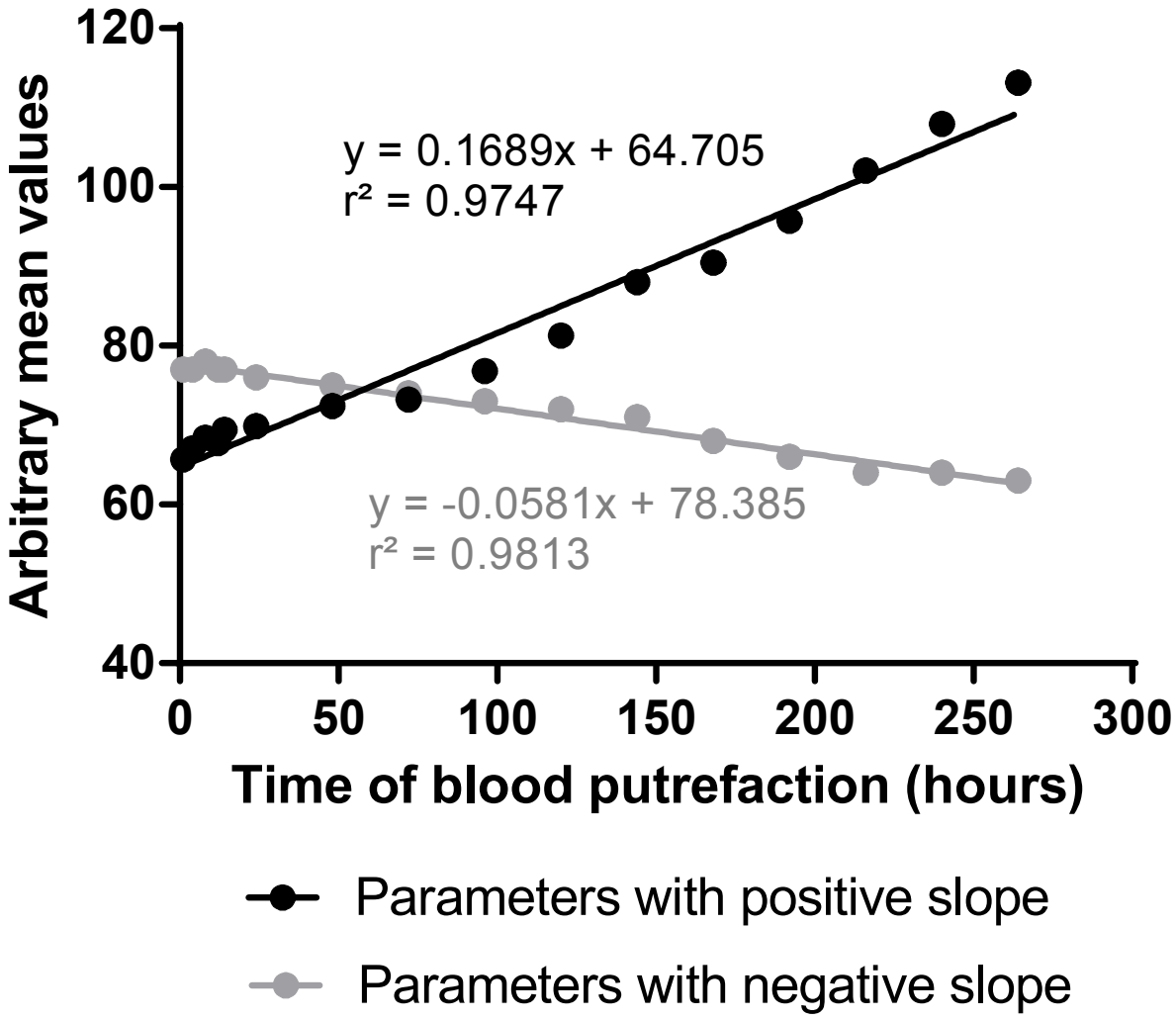

Figure 2

A

$$PMI = \frac{(64.71 - \left|\overline{Y}_X\right|)}{0.17} \pm 2.16 \times \left[77.60 \times \sqrt{0.08 + \frac{(\overline{Y}_X + 81.84)^2}{3631.78}} \right]$$

B

$$PMI = -\frac{(78.38 - \left|\overline{Y}_X\right|)}{0.06} \pm 2.16 \times \left[-73.86 \times \sqrt{0.08 + \frac{(\overline{Y}_X + 72.49)^2}{429.69}} \right]$$

C

$$s_x = \frac{s_y}{m} \sqrt{\frac{1}{K} + \frac{1}{n} + \frac{(\overline{Y}_X - \overline{y})^2}{m^2 \sum xx}}$$

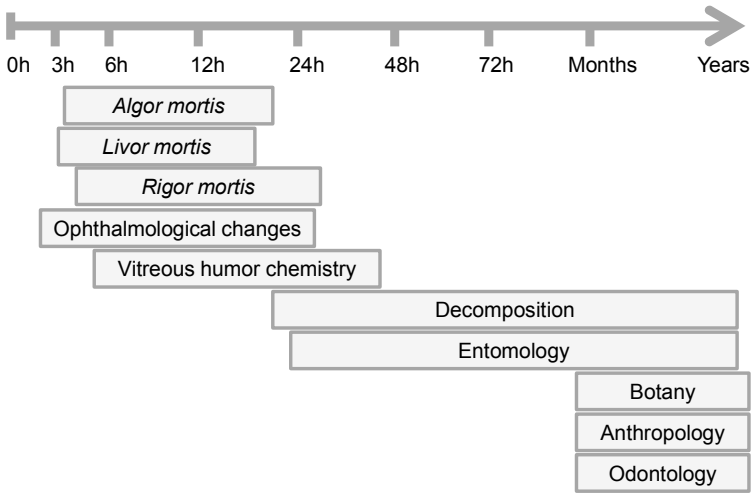

Abstract Figure - Schematic representation of methods to estimate postmortem interval.

- A linear correlation between blood putrefaction time and biochemical parameters concentrations was obtained.
- Total and direct bilirubin, urea, uric acid, transferrin, IgM, CK, AST, calcium and iron shown to be promising.
- Two mathematical models that may have predictive value for estimation of the *postmortem interval* were developed.
- Obtained results might be complementary procedures for the methodologies already used.